doi: 10.56761/EFRE2024.S4-P-004304

Experimental research on friction of sheet metal forming by superimposing ultrasonic vibrations

Lijun Wu[1,], Mikhail D. Starostenkov[2], Zhuoyun Yang[1], Haixiang Wang[1], Miaoyan Cao[1], Guojiang Dong[1]*

[1]*Yanshan University, Qinhuangdao, China*
[2]*Polzunov Altai State Technical University, Barnaul, Russia*
[*]*lijunysu@gmail.com*

Abstract. In sheet metal forming, the friction between sheet metal and tools can be reduced by ultrasonic vibration (UV), and the forming performance can be improved by the surface effect. In this study, a new friction test apparatus to determine the effect of UV on the friction coefficient is designed and fabricated, including relative parallel and rotational motion between sheet and punch. Ultrasonic vibrations are applied on two 40Cr punches at a frequency of 20 kHz. Several groups of tests were conducted under different conditions, sheet metals of stainless steel 304 are utilized for the tests. The friction coefficient is decreased by approximately 40% in parallel motion test, and by approximately 80% in rotational motion test.
Keywords: ultrasonic vibration, sheet metal forming, friction.

1. Introduction

Friction is the most significant factor influencing the quality of the sheet metal forming (SMF), which affects the energy needed to deform a sheet material, the stresses and strains in the workpiece material and, hence, the quality of the product [1, 2]. Ultrasonic vibration (UV) has been introduced for friction reduction in SMF, as shown in Fig. 1. Jimma et al. [3] found that excitation of UV energy at frequencies of 20 and 28 kHz leads to lower friction and material deformation resistance values. Huang et al. [4] performed an experimental study to determine the influence of UV on the micro deep drawing process to improve formability and showed that the limiting drawing ratio in stainless steel foils can be obviously improved. Vibrations of different frequencies have been applied in various types of sliding surfaces, as shown in Fig. 2. Types 1 and 2 are vibrations that are longitudinal and transverse to the macroscopic sliding direction, respectively, while type 3 is an out-of-plane vibration. Usually, vibrations are applied to only one of the two surfaces, such as block A in Fig. 2.

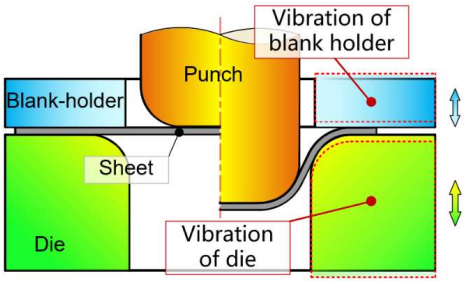

Fig. 1. Ultrasonic vibrations superposition in SMF

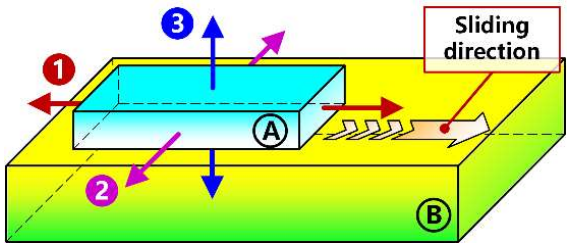

Fig. 2. Types of applying vibration.

Littmann et al. [5] used a 60 kHz piezoelectric actuator sliding on a guide track (type 1), the applied vibration is parallel to the relative sliding direction. Kumar and Hutchings [6] applied ultrasonic vibrations as types 1 and 2. They concluded that longitudinal vibrations (type 1) are more effective at friction reduction than transverse vibrations and that the velocity ratio greatly influences friction reduction. Popov et al. [7] investigated the influence of out-of-plane ultrasonic vibrations (type 3) on different material combinations and discovered that ultrasonic vibrations create less friction reduction on soft materials than on hard materials.

Despite the abovementioned achievements in friction reduction by superimposing ultrasonic vibrations, most of this research has been focused on the relative parallel motion between contact pairs (as shown in Fig. 2). Many studies [2, 8] have proven that the friction force at the die radius region (as shown in Fig. 1) has a great share of the entire process force. In this study, a new friction test apparatus to determine the effect of UV on the friction coefficient is designed and fabricated, including relative parallel and rotational motion between sheet and tools. With the test apparatus, several groups of tests can be conducted under different conditions to explore the friction characteristics of SMF by superimposing ultrasonic vibrations.

2. Experimental setups and Material

Schematic diagrams and photos of the friction test apparatuses for parallel and rotational motions are shown in Fig. 3a and 3b, respectively.

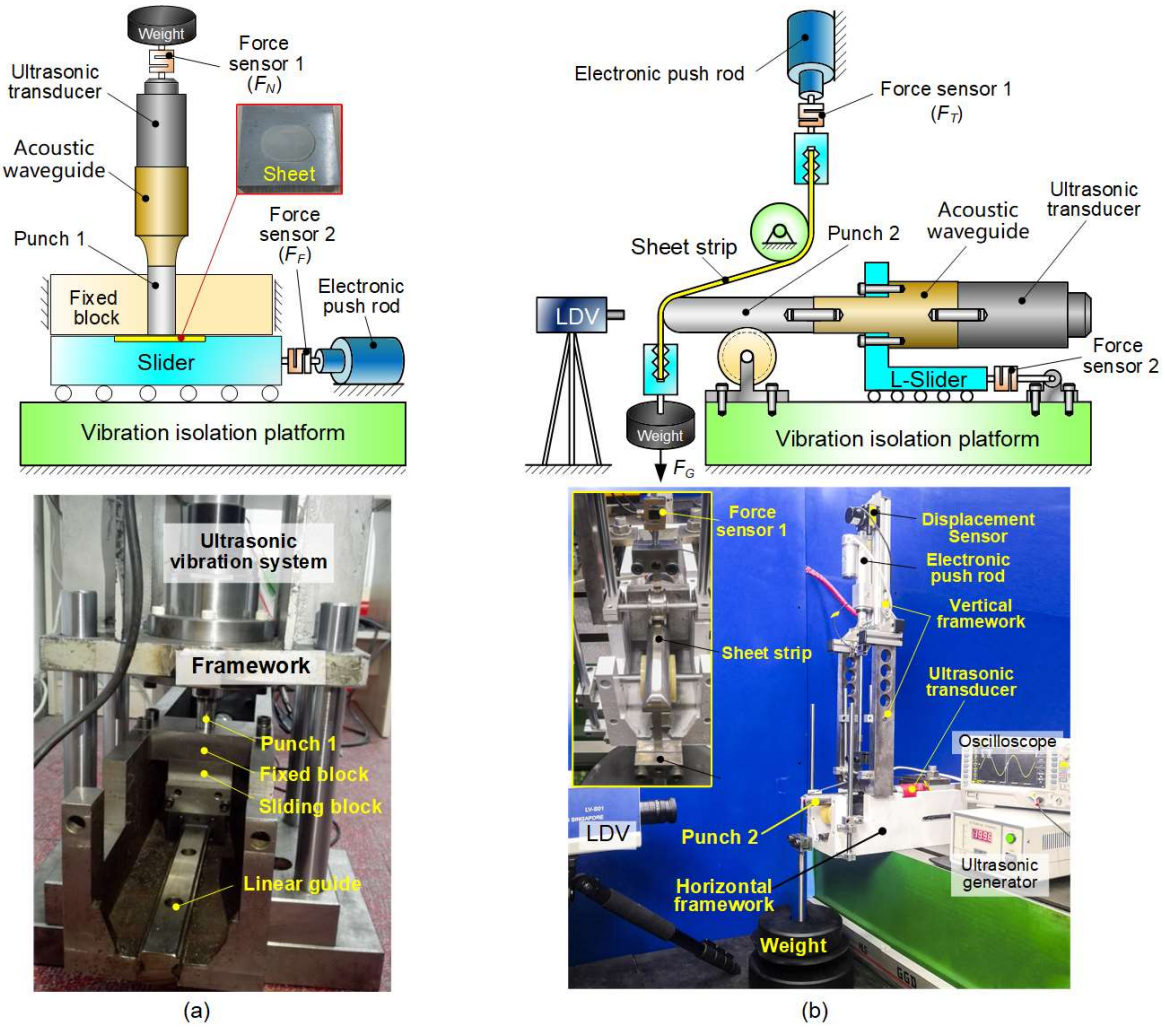

(a) (b)

Fig. 3. Schematic diagrams and photos of the friction tests: (a) parallel motion; (b) rotational motion.

2.1. Friction test setup for parallel motion

As shown in Fig. 3a, the main parts of the test system include: (1) the ultrasonic generator, which is connected to the sandwich piezoelectric ceramic ultrasonic transducer; (2) the stepped cylindrical acoustic waveguide is mounted between the transducer and the punch 1 to magnify the transmitted vibration amplitude and is made of the same material as the punch 1 to achieve an optimum wave

transition; (3) The punch 1 made of 40Cr is perpendicular to the sheet embedded into the groove of the sliding block, the dimensions and amplitude distribution are shown in Fig.4 (a); (4) the fixed block, which can effectively improve perpendicularity between punch 1 and sheet; (5) the sliding block, which can move horizontally along the linear guide under the action of the electronic push rod; (6) the electrical push rod, whose speed can be adjusted between 0 and 5 mm/s; and (7) the force sensor 1 and force sensor 2, the two sensors have the same specifications with a natural frequency of 64 kHz and dynamic response frequency of 2500 Hz. The two sensors can directly measure the normal force and the tangential force in UV conditions due to its natural frequency (nearly 3 times larger than 20 kHz) and high dynamic response frequency.

Therefore, the normal load from the weight (denoted by F_N) can be measured by force sensor 1, which provides a mean nominal contact pressure on the flat end of the punch. Ultrasonic vibrations and sliding movements are perpendicular to each other. The punch 1 is pressed against the surface of sheet embedded in the sliding box, hence the sheet can move at different velocities with the electrical push rod. The sliding block is supported by high-precision linear guides, and the frictional force (denoted by F_F) can be measured by force sensor 2 that is attached to the sliding block. The outputs from the two force sensors are digitized and recorded in a PC, and the friction coefficient in the parallel motion test can be expressed as

$$\mu_p = \frac{F_F}{F_N}, \tag{1}$$

where μ_p stands for friction coefficient in parallel motion test.

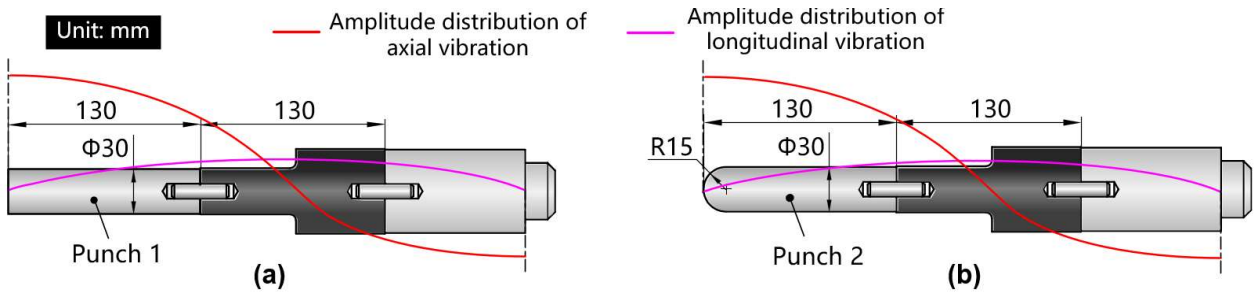

Fig. 4. Dimensions and amplitude distribution: (a) punch 1; (b) punch 2.

2.2. Friction test setup for rotational motion

As shown in Fig. 3b, main parts of the test system include: (1) the horizontal framework is fixed on the vibration isolation platform, and the vertical framework is fixed on the horizontal frame; (2) the electronic push rod is fastened to the vertical frame, and its velocity can be adjusted between 0 mm/s and 5 mm/s; (3) The punch 2 made of 40Cr, its dimensions and amplitude distribution are shown in Fig. 4b; (4) the displacement sensor acquires the displacement data of the electronic push rod, and the actual velocity of the rod can be calculated simultaneously; (5) the force sensor 1 and force sensor 2, with the same specification as that in parallel motion test setup, force sensor 1 can measure the tensile force of the sheet strip (denoted by F_T), and force sensor 2 can measure the axial force of the vibration components. (6) the weight, pulled upward through the tightened sheet strip, the tensile force of sheet strip below the punch 2 (sheet strip which has not contacted with punch 2), represented by F_G, equals to the gravity of the weight.

In rotational motion tests, the friction force between sheet strip and the punch top follows Coulomb's law, and μ_r, defined as friction coefficient, is assumed to be a constant value throughout the contact area. As shown in Fig. 5, the wrap angle is represented by α, previous study [9] has deduced the expression, yields

$$\mu_r = \frac{1}{\alpha} \ln \frac{F_T}{F_G}, \tag{2}$$

where μ_r stands for friction coefficient in rotational motion test.

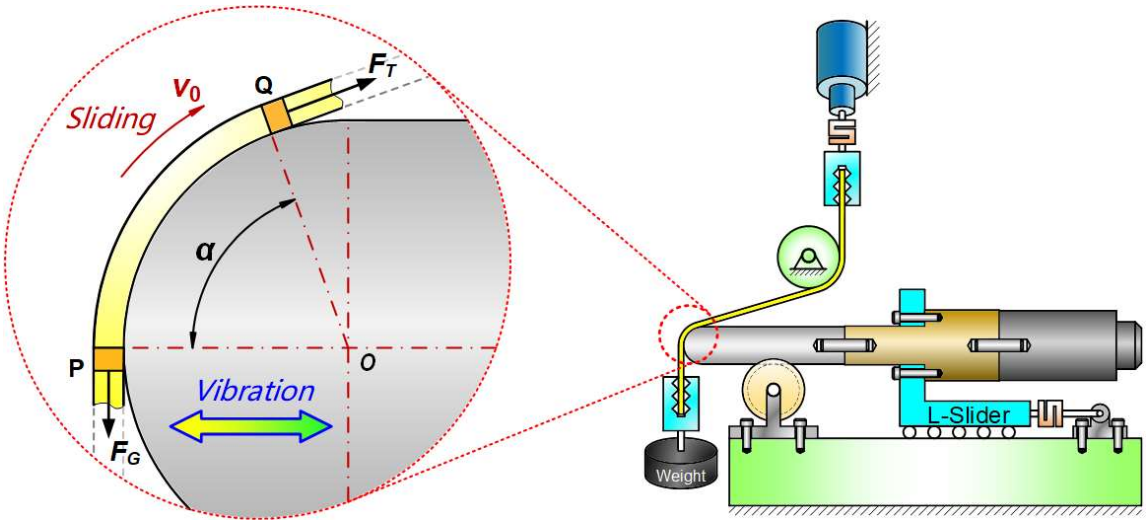

Fig. 5. Force analysis of punch 2.

2.3. Material of sheet metals

Stainless steel 304 (SS304) is chosen for the friction tests. Blank sheets with a thickness of 1 mm are prepared by wire cutting for parallel motion tests, where the workpieces are mounted into the grooves of the slider as shown in Fig. 3a. In the rotational motion tests, the width of all sheet strips is 10 mm and the thickness of 0.1 mm is adopted for SS304 strips. The mechanical properties of SS304 at room temperature are listed in Table 1.

Table 1. Mechanical Properties of SS304 sheet (at room temperature)

Properties	Values
Hardness, Rockwell B [–]	≤ 92
Tensile Strength, Ultimate [MPa]	≥ 615
Tensile Strength, Yield [MPa]	≥ 205
Elongation at Break [–]	38 ~ 42%
Modulus of Elasticity [GPa]	193
Poisson's Ratio [–]	0.29
Shear Modulus [MPa]	77

3. Results and discussion

3.1. Parallel motion tests

Fig. 6 shows the curves of the friction forces versus sliding displacement (F_F–F_N) with different normal loads, and the relative sliding velocities (denoted by v_{rel}) are all set to 1 mm/s. When a certain normal load is applied, the friction forces increase rapidly from zero to their maximum values and then gradually decrease to a constant because the friction coefficient of the static contact at the beginning of sliding is higher than that of the dynamic contact.

The friction force at a specified normal load can be obtained using the average value of the friction force curves from the samples. Fig. 7 shows the F_F–F_N curves at different relative sliding velocities. The favorable linearity between friction forces and contact loads can be observed from the curves, accordingly, the dynamic friction coefficients are constant.

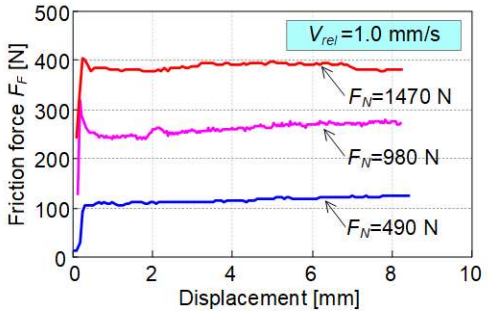

Fig. 6. Curves of friction force versus displacement.

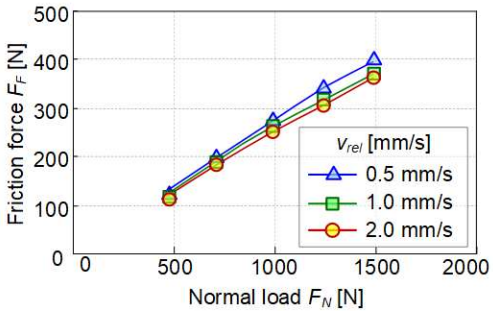

Fig. 7. Curves of friction force versus normal load.

Fig. 8 shows the changing tendency of friction coefficient μ_p versus sliding displacement by superimposing ultrasonic vibrations, and the whole test can be divided into two periods: sliding without UV, and sliding with UV. The values of μ_p fluctuates according to sliding displacement, the average value of μ_p is reduced from 0.274 to 0.168 when ultrasonic vibrations are applied, and the reduction ratio is approximately 40%. Fig. 9 shows the μ_p–F_N curves at different sliding velocities. With the superimposed ultrasonic vibrations, the values of μ_p are nearly the same at three different sliding velocities, and friction decreases along with the increasing of sliding velocity.

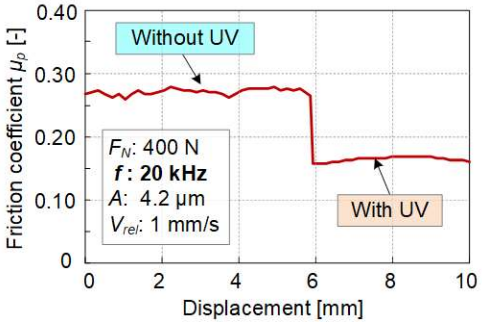

Fig. 8. Curve of friction coefficient versus displacement.

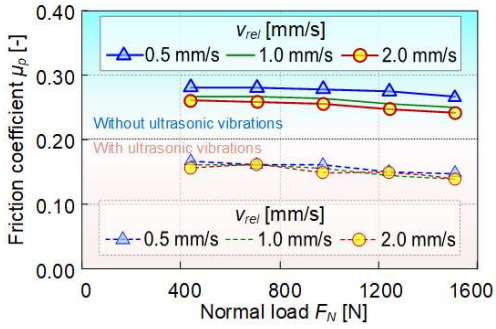

Fig. 9. Curves of friction coefficient versus normal load.

3.2. Rotational motion tests

Fig. 10a and 10b plot the time-dependent curves of the instant friction coefficient μ_r, calculated using Eq. (2) under different experimental conditions.

Fig. 10a shows the results of one test using strips of stainless steel 304 (the mechanical properties are listed in Table 1) under UV conditions. The vibration frequency, f, is 20 kHz; the vibration amplitude, A, measured by LDV is 8.87 μm; the wrap angle α is set to 1.46 (84°); the weight G is 10 kg, and the sliding velocity, v_0, is set to 0.5 mm/s. The whole test can also be divided into two periods: sliding without UV, and sliding with UV. The average value of μ_r is reduced from 0.2047 to 0.0246 when ultrasonic vibrations are applied, the reduction ratio reaches approximately 87.98%.

Fig. 10b plots the results of tests under the same parameters as Fig. 10a, except for the sliding velocity, v_0, which was increased from 0.5 mm/s to 1 mm/s. The average value of μ_r is reduced from 0.2085 to 0.0326 when ultrasonic vibrations are superimposed, and the reduction ratio is approximately 84.36%.

Fig. 11a show the effect of velocity the sliding velocity v_0 on friction coefficient μ_r. The tests are carried out with different wrap angles (α = 84°), the same weight (G = 10 kg), and the same frequency and amplitude of superposed vibrations (f = 20 kHz, A = 8.87 μm). The sliding velocity v_0 of 0.5, 1, 2, 3 and 4 mm/s are employed respectively. It can be observed that the sliding velocity have no

obvious influence on friction coefficient, under both without UV and with UV test conditions. Fig. 11b show the effect of amplitude on friction coefficient μ_r, and the values of 8.87, 11.22, 12.72 and 15.27 μm are chosen for tests, respectively. A slight increase along with the enlargement of amplitude can be observed from the two curves, because the larger amplitude of UV means larger power output, and leads to more severe wear and friction between punch and sheet metal.

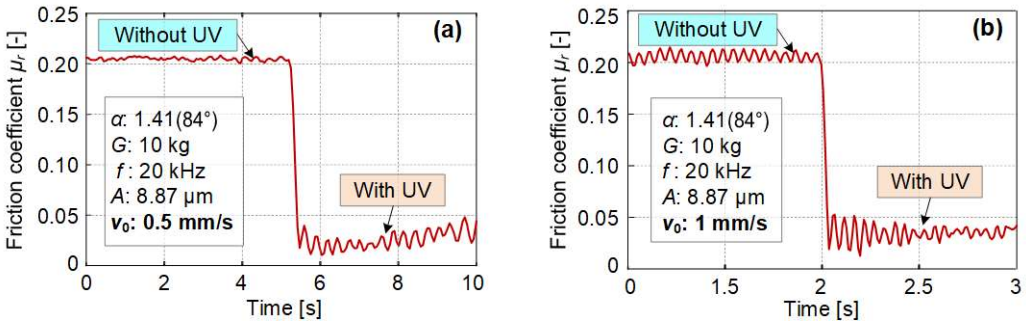

Fig. 10. Time-dependent curves of friction coefficient at: (a) v_0 = 0.5 mm/s; (b) v_0 = 1 mm/s.

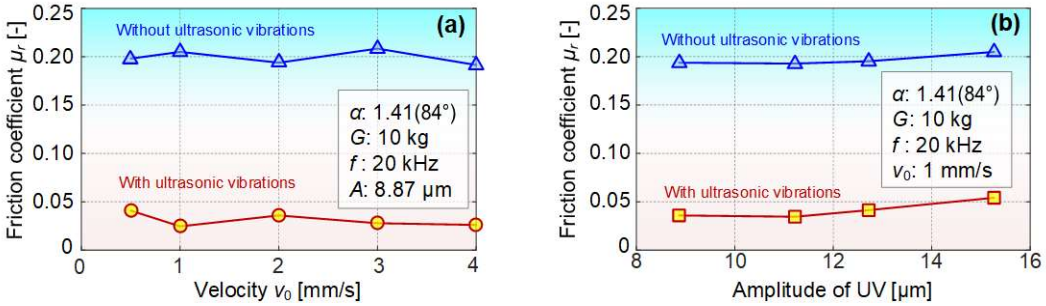

Fig. 11. Curves of friction coefficient versus: (a) velocity v_0; (b) amplitude of UV.

4. Conclusion

First, a new friction test apparatus that could determine the effect of UV on the friction coefficient including parallel motion and rotational motion is designed and fabricated, and using the apparatus, several groups of tests are carried out under different conditions.

Second, in both parallel motion and rotational motion tests, significant reduction of friction coefficient can be observed by superimposing UV. The average reduction ratio of approximately 40% can be obtained in parallel motion test. In rotational motion tests, because one of surface of sheet is free, the average value of reduction ratio reaches approximately 80%.

Third, the sliding velocity has no significant influence on the reduction of friction coefficient in both parallel motion and rotational motion tests. The increase of amplitude of UV leads to more severe wear and friction between punch and sheet metal.

Acknowledgement

The work was supported by the National Natural Science Foundation of China (52175367, 51775480) and the Natural Science Foundation of Hebei Province (E2018203339).

5. References

[1] L. Figueiredo, A. Ramalho, M.C. Oliveira, L.F. Menezes, Experimental study of friction in sheet metal forming, *Wear*, vol. **271**, 1651, 2011; doi: 10.1016/j.wear.2011.02.020

[2] P.L. Menezes, K. Kumar, Kishore, et al, Influence of friction during forming processes–a study using a numerical simulation technique. *Int. J. Adv. Manuf. Technol.*, vol. **40**, 1067, 2008; doi: 10.1007/s00170-008-1425-5
[3] T. Jimma, Y. Kasuga, N. Iwaki, et.al, An application of ultrasonic vibration to the deep drawing process, *J. Mater. Process. Technol.*, vol. **80–81**, 406, 1998; doi: 10.1016/S0924-0136(98)00195-2
[4] Y.M. Huang, Y.S. Wu, J.Y. Huang, The influence of ultrasonic vibration-assisted micro-deep drawing process, *Int. J. Adv. Manuf. Technol.*, vol. **71**, 1455, 2014; doi: 10.1007/s00170-013-5553-1
[5] W. Littmann, H. Storck, J. Wallaschek, Sliding friction in the presence of ultrasonic oscillations: superposition of longitudinal oscillations, *Archive of Applied Mechanics*, vol. **71**, 549, 2001; doi: 10.1007/s004190100160
[6] V.C. Kumar, I.M. Hutchings, Reduction of the sliding friction of metals by the application of longitudinal or transverse ultrasonic vibration, *Tribology International*, vol. **37**, 833, 2004; doi: 10.1016/j.triboint.2004.05.003
[7] V.L. Popov, J. Starcevic, A.E. Filippov, Influence of Ultrasonic In-Plane Oscillations on Static and Sliding Friction and Intrinsic Length Scale of Dry Friction Processes, *Tribology Letters*, vol **9**, 25, Oct. 2009; doi: 10.1007/s11249-009-9531-6
[8] Y. Ashida, H. Aoyama, Press forming using ultrasonic vibration, *J. Mater. Process. Technol.*, vol. **187**, 118, Nov. 2006; doi: 10.1016/j.jmatprotec.2006.11.174
[9] L.J. Wu, C.C. Zhao, M.Y. Cao, et. al, Effect of ultrasonic and low frequency vibrations on friction coefficient at die radius in deep drawing process, *Journal of Manufacturing Processes*, vol. **71**, 56, Sep. 2021; doi: 10.1016/j.jmapro.2021.09.008